

LETTER • OPEN ACCESS

## Synchronous spring precipitation in Southeastern China and Bengal: a potential indicator for the Indian summer monsoon?

To cite this article: Keyan Fang *et al* 2024 *Environ. Res. Lett.* **19** 104008

View the [article online](#) for updates and enhancements.

### You may also like

- [Impact of cloud radiative heating on East Asian summer monsoon circulation](#)  
Zhun Guo, Tianjun Zhou, Minghui Wang *et al.*
- [Disentangling physical and dynamical drivers of the 2016/17 record-breaking warm winter in China](#)  
Tuantuan Zhang, Yi Deng, Junwen Chen *et al.*
- [Drying trend in land and sea in East Asia during the warm season over the past four decades](#)  
Go-Un Kim, Hyoeun Oh and Jin-Yong Jeong



The Electrochemical Society  
Advancing solid state & electrochemical science & technology

# UNITED THROUGH SCIENCE & TECHNOLOGY

## 248th ECS Meeting Chicago, IL October 12-16, 2025 *Hilton Chicago*



## Science + Technology + YOU!

## SUBMIT ABSTRACTS by March 28, 2025

[SUBMIT NOW](#)

ENVIRONMENTAL RESEARCH  
LETTERS

## LETTER

## OPEN ACCESS

RECEIVED  
8 April 2024REVISED  
21 July 2024ACCEPTED FOR PUBLICATION  
14 August 2024PUBLISHED  
28 August 2024

Original content from  
this work may be used  
under the terms of the  
[Creative Commons  
Attribution 4.0 licence](#).

Any further distribution  
of this work must  
maintain attribution to  
the author(s) and the title  
of the work, journal  
citation and DOI.



## Synchronous spring precipitation in Southeastern China and Bengal: a potential indicator for the Indian summer monsoon?

Keyan Fang<sup>1,\*</sup> , Feifei Zhou<sup>1</sup>, Hao Wu<sup>1,2</sup>, Hui Tang<sup>3</sup>, Zepeng Mei<sup>1</sup>, Jinbao Li<sup>4</sup>, Tinghai Ou<sup>5</sup>, Zheng Zhao<sup>1</sup> and Deliang Chen<sup>5</sup> <sup>1</sup> Key Laboratory of Humid Subtropical Eco-geographical Process (Ministry of Education), College of Geographical Sciences, Fujian Normal University, Fuzhou 350007, People's Republic of China<sup>2</sup> State Key Laboratory of Nuclear Resources and Environment, East China University of Technology, Nanchang 330013, Jiangxi, People's Republic of China<sup>3</sup> Department of Geosciences, University of Oslo, Oslo, Norway<sup>4</sup> Department of Geography, University of Hong Kong, Hong Kong Special Administrative Region of China, People's Republic of China<sup>5</sup> Regional Climate Group, Department of Earth Sciences, University of Gothenburg, Gothenburg 460, Sweden

\* Author to whom any correspondence should be addressed.

E-mail: [kujanfang@gmail.com](mailto:kujanfang@gmail.com)**Keywords:** spring synchronous precipitation, East Asian Subtropical Jet (EASJ), El Niño–Southern oscillation (ENSO), Indian summer monsoon (ISM), tree ringSupplementary material for this article is available [online](#)

## Abstract

Spring precipitation in southeastern China and Bengal, occurring during the transitional phase from winter to summer monsoons, serves as a critical window into the dynamics of large-scale circulations and the subsequent summer monsoon. While many studies have analyzed spring precipitation in southeastern China and Bengal, their interconnections and implications for the summer monsoon have remained relatively under explored. We utilized the Empirical Orthogonal Function of spring precipitation to reveal Synchronous Spring Precipitation (SSP) in southeastern China and Bengal. This synchronicity is bridged by the East Asian Subtropical Jet (EASJ) that extends from Bengal to southeastern China. The EASJ was predominantly correlated with precipitation in southeastern China prior to the 1990s, while it developed a more profound connection with precipitation in Bengal after the 1990s. Notably, SSP anomalies occurred during the developing phase of the El Niño–Southern Oscillation (ENSO). The predictive capacity of SSP for the Indian summer monsoon (ISM) amplifies during periods of the intensified SSP–ENSO correlations and positive phase of the North Pacific Meridional Mode. Tree-ring based reconstructions spanning the past two centuries further corroborate the persistent linkages among the SSP, ISM, and ENSO. Our research sheds light on the intricate interplay of these factors and their significance in understanding and predicting the monsoon dynamics in the region.

## 1. Introduction

Spring precipitation bridges the winter and summer climates and plays a pivotal role in ecological processes and agricultural activities, primarily due to its alignment with the onset of the plant growing season (Tian and Yasunari 1998, Wang *et al* 2002, Wan and Wu 2007, Tang *et al* 2022, Chen *et al* 2023). The spring climates were considered as precursors of the following Indian summer monsoon (ISM), including the Eurasian snow cover, the El Niño–Southern Oscillation (ENSO), wind and pressure

modes (Kumar *et al* 1999, Kakade and Kulkarni 2016, Hari *et al* 2022). However, it is unclear about the predictability of the spring precipitation on the ISM. In contrast to the summer monsoon rainfall that has been extensively studied (Kumar *et al* 1999, Wang and Ding 2008, Wang *et al* 2017, Hari *et al* 2022), changes in spring precipitation in southern and eastern Asia are less understood.

The spring precipitation in southeastern China is recognized as the second most influential weather system in China (Tian and Yasunari 1998, Huijun *et al* 2002, Chen *et al* 2014, 2023, Zhu *et al* 2014,

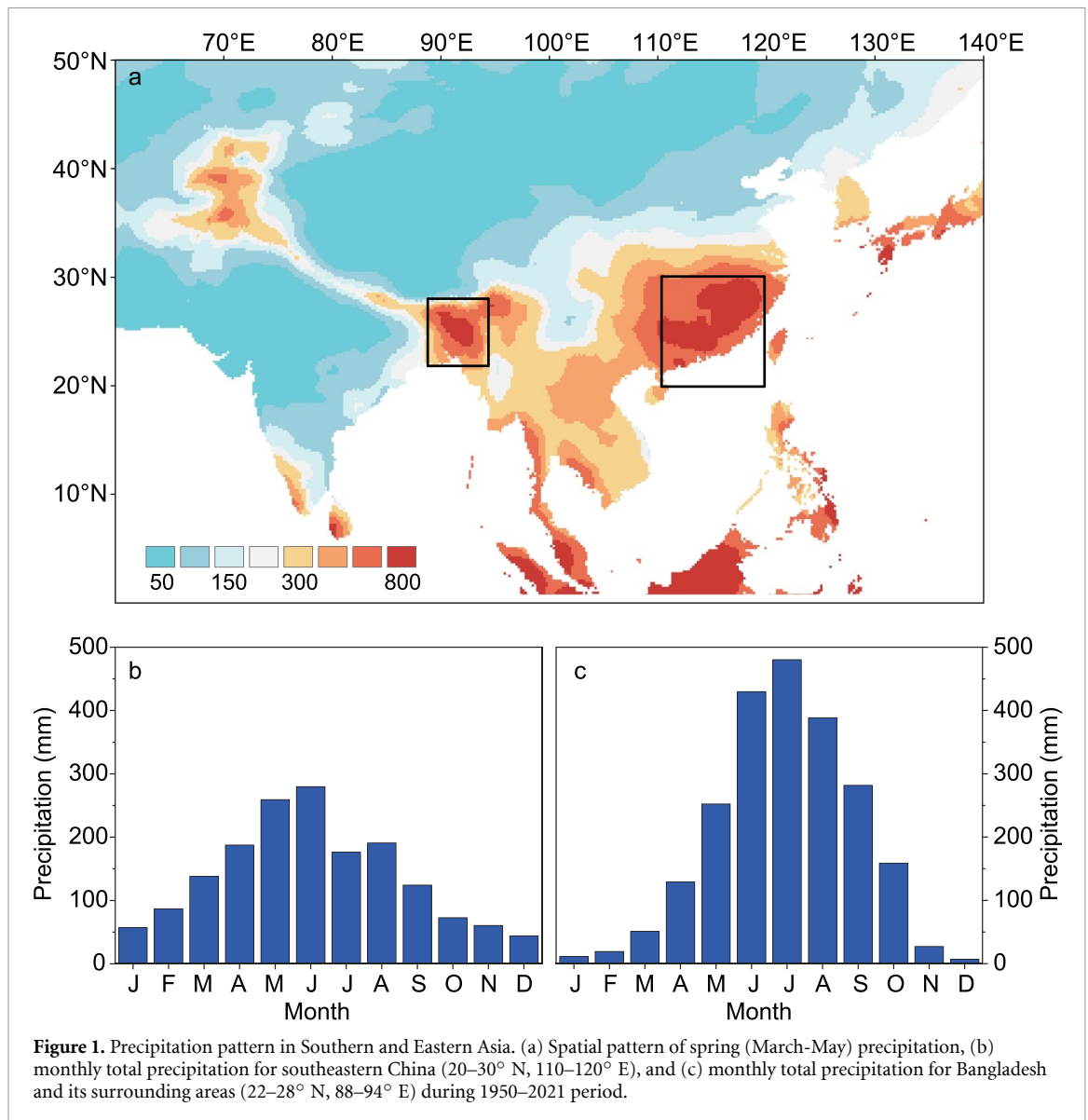


**Figure 1.** Precipitation pattern in Southern and Eastern Asia. (a) Spatial pattern of spring (March–May) precipitation, (b) monthly total precipitation for southeastern China (20–30° N, 110–120° E), and (c) monthly total precipitation for Bangladesh and its surrounding areas (22–28° N, 88–94° E) during 1950–2021 period.

Li *et al* 2020, Luo *et al* 2020, Wang *et al* 2021), occurring predominantly from March to May, and accounts for 40%–60% of the annual precipitation centered in Fujian and Guangdong provinces in southeast China (figure 1). The spring precipitation in southeastern China is closely linked to the pre-summer precipitation from April to June centered in Guangdong and Guangxi provinces (Li *et al* 2020, Luo *et al* 2020). Several studies have revealed the thermal and dynamic effects of the Tibetan Plateau on the spring precipitation in southeastern China, particularly through the East Asian Subtropical Jet (EASJ) (Wan and Wu 2007, Wang *et al* 2021). The EASJ is generally positively correlated with the spring precipitation in southeastern China (Huang *et al* 2015, Wang *et al* 2021). Others suggest that the western Pacific Subtropical High can enhance the spring precipitation via increased moisture transport from ocean to southeastern China (Tian and Yasunari 1998, Zhu *et al* 2014).

Apart from southeastern China, Bengal stands out for its substantial extratropical spring precipitation, with spring rainfall levels nearly ten times greater than in winter (figure 1). The spring and summer climate in eastern Asia and the ISM domain are modulated by the interconnected ENSO, western Pacific Subtropical High and EASJ, which showed a regime shift around 1990 (Huang *et al* 2018, Li and Wang 2013). It is intriguing to explore whether there exists interconnection between spring precipitation in southeastern China and Bengal and their time-varying relationships with the ISM.

## 2. Methods

### 2.1. Climate and tree-ring data

We utilized monthly Climate Research Unit (CRU TS4.06) land temperature and precipitation data in southern and eastern Asia (0–50° N, 60–140° E), which spans from 1901 to 2021 with a grid resolution

of  $0.5^\circ \times 0.5^\circ$  (Harris *et al* 2020). To ensure the robustness of our analysis, we focused on post-1950 data, as comprehensive meteorological data become available after 1950 (Cook *et al* 2010). To discern climate patterns associated with oceanic and atmospheric conditions, we conducted an extensive analysis of the regional climate data in relation to SST, Geopotential Height, and near-surface (10 m) wind speed. For the SST data, we incorporated the HadISST dataset, which offers a spatial resolution of  $1^\circ \times 1^\circ$  and spans from 1870 onwards (Rayner *et al* 2003). Regarding Geopotential Height and wind data, we relied on the European Center for Medium-Range Weather Forecasting (ECMWF) Reanalysis version 5 (ERA5). This dataset provides hourly estimates of climate variables from 1940 to the present day (Hersbach *et al* 2023). To characterize the Indian summer monsoon (ISM), we employed the homogeneous Indian monthly rainfall datasets spanning from 1871 to 2016. In our analysis, we employed the well-recognized Niño 3.4 and Niño 4 index to characterize the ENSO (Trenberth and Stepaniak 2001), extending from 1871 to 2022.

To assess the stability of spring precipitation regimes, we harnessed the invaluable attributes of tree rings, which offer precise dating, high resolution, and strong climate sensitivity (Frank *et al* 2022). Our dataset incorporates tree-ring data obtained from 167 subtropical sites ( $15\text{--}35^\circ$  N,  $80\text{--}130^\circ$  E). Among these, 142 samples were obtained from the International Tree-Ring Data Bank (ITRDB), with an additional 25 samples collected by our research team (table S1). To ensure the integrity of our tree-ring data, we detrended by fitting a negative exponential curve and subsequently constructed chronologies using a biweight robust mean (Cook 1985).

## 2.2. Statistical and reconstruction methods

In our study, we employed the widely recognized EOF analysis to identify the dominant spatial patterns of spring precipitation. Prominent EOF modes and their corresponding time series are typically regarded as key indicators of climate patterns (Lorenz 1956). To evaluate time-varying correlations across different timescales, we utilized Wavelet coherence (Grinsted *et al* 2004). This approach involves breaking down time series data into various temporal components through wavelet analysis and subsequently calculating localized correlations, allowing to gain insight into the evolving relationships between variables across different timescales. Running correlations, specifically 21 year moving window correlations, are utilized to examine the temporal variations in the relationships between SSP and ISM, as well as ENSO.

We applied the principal components regression approach for our tree-ring-based climate reconstructions (Cook *et al* 2010). This involved the selection of the tree-ring chronologies that exhibited significant correlations with the target climate variables, which

were then used to extract principal components for climate reconstruction. The model's effectiveness was ascertained by the leave-one-out cross-validation technique (Michaelsen 1987), which is particularly well-suited for situations with short observational data.

## 3. Results

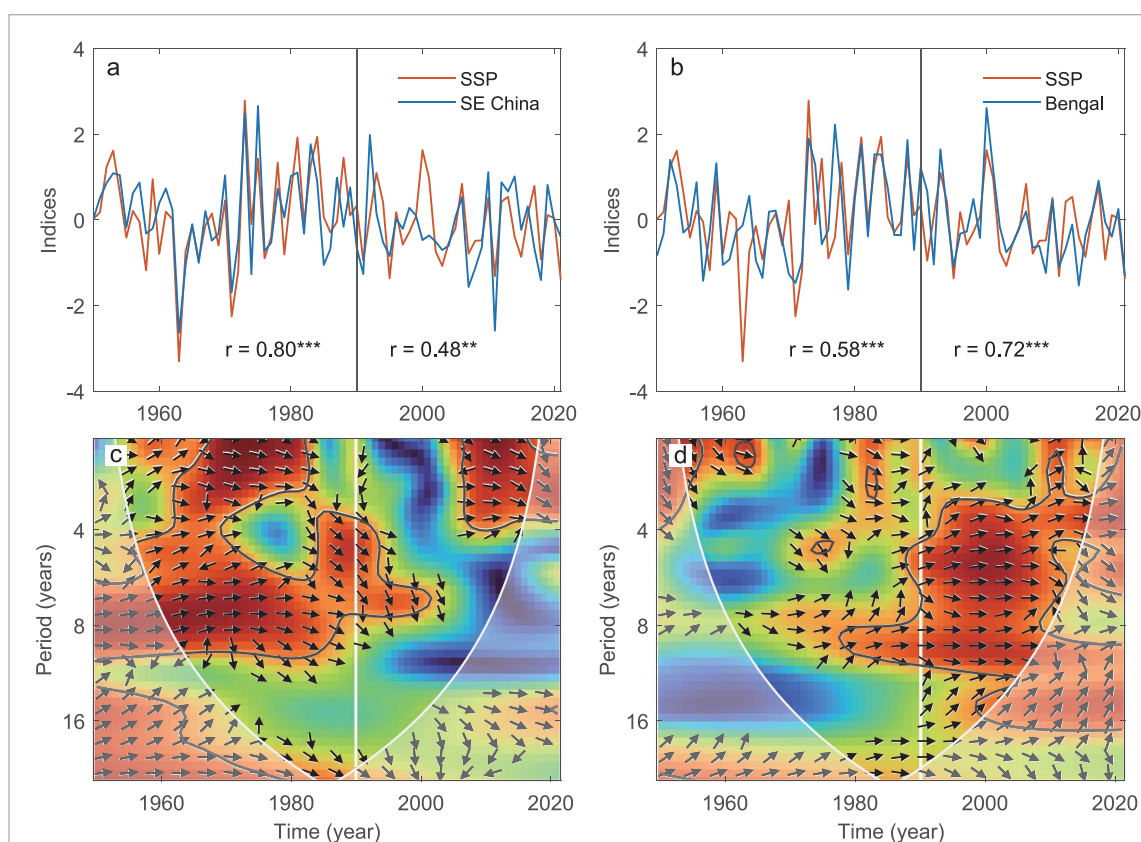
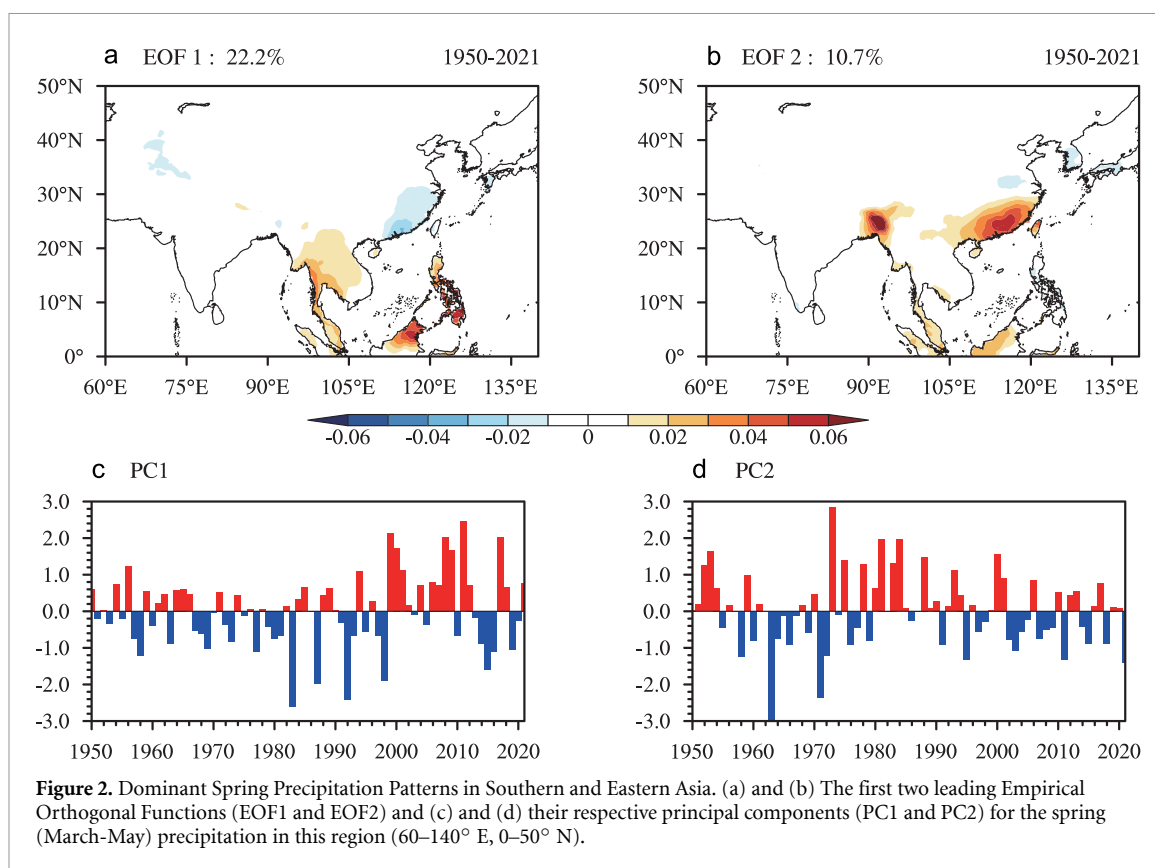
### 3.1. Synchronous spring precipitation (SSP) and its linkages with the EASJ

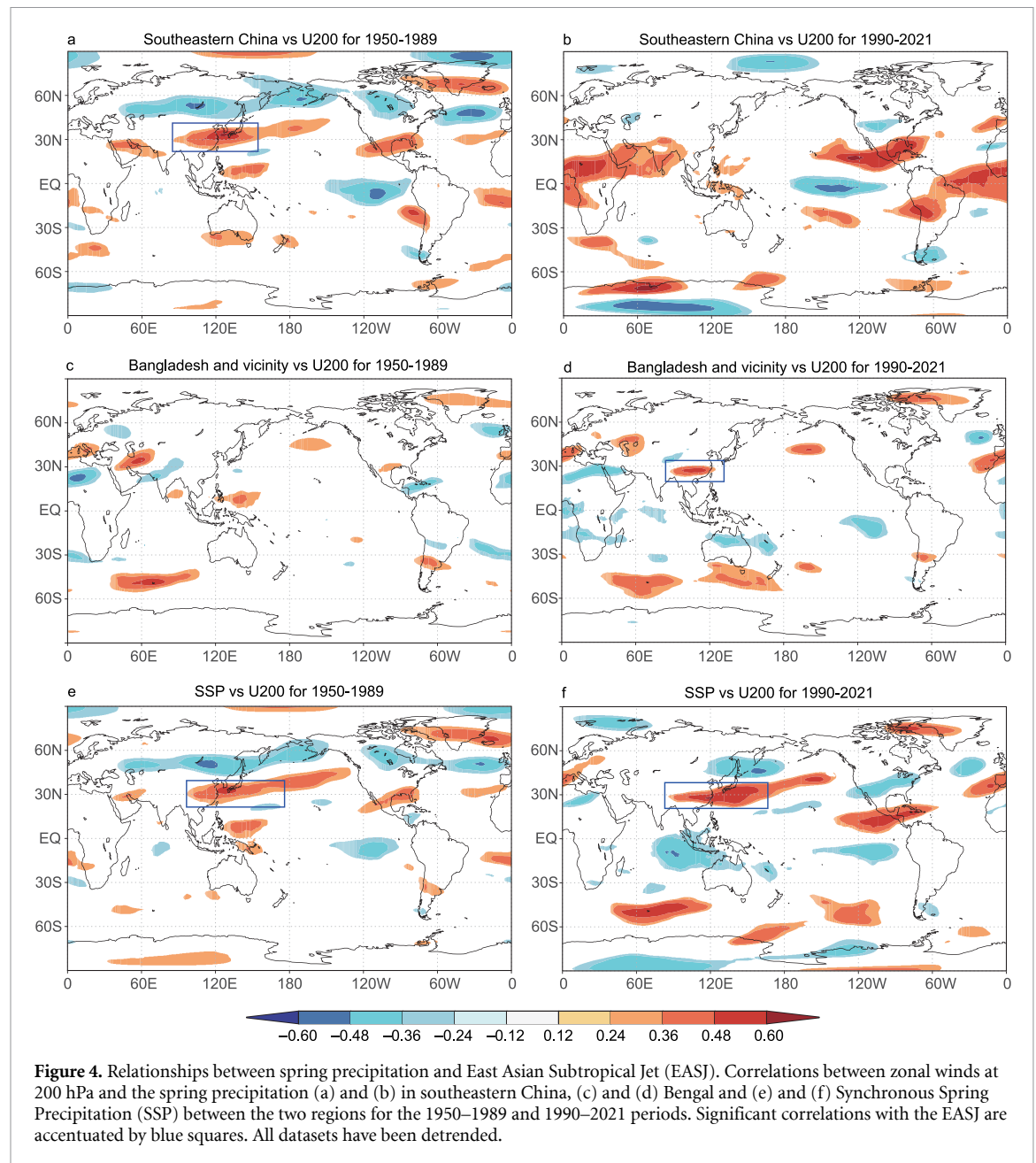
The leading empirical orthogonal function (EOF1) associated with spring precipitation accounts for 22.2% of the total variance and exhibits its highest loadings over the Philippines and the surrounding regions (figure 2(a)). On the other hand, EOF2 explains 10.7% of the variance and displays significant loadings in southeastern China and Bengal (figure 2(b)). The first 2 modes passed the North test with a confidence level of 95% (figure S1). Our particular focus is on EOF2, as it provides a clear representation of SSP between southeastern China and Bengal. Accordingly, we leverage the EOF2 for our SSP analysis. The SSP between southeastern China and Bengal is also observed for the global domain (figure S2). Notably, the SSP experienced a notable historical trajectory, hitting its lowest point in the 1960s, reaching its peak in the 1970s, and subsequently declining since then (figure 2(d)). This trend, characterized by decreasing spring precipitation and a narrowing range of variability in recent years, aligns with the findings of earlier studies on spring precipitation in southeastern China (Li and Wang 2013, Tang *et al* 2022).

Prior to approximately 1990, spring precipitation in southeastern China was closely associated with the SSP, as substantiated by their strong correlations (figures 3(a) and (c)). However, a noteworthy shift occurred after 1990, where correlations with precipitation in southeastern China weakened, while those with Bengal's precipitation intensified (figures 3(b) and (d)). This regime shifts around 1990 is also evident in correlations with the East Asian Subtropical Jet (EASJ) (figure 4). Before the regime shift around 1990, precipitation in southeastern China exhibited significant correlations with the EASJ, as indicated by strong zonal wind associations at 200 hPa over eastern subtropical Asia (figure 4(a)). However, these correlations vanished after 1990 (figure 4(b)). In contrast, Bengal's precipitation showed no significant correlations ( $p < 0.1$ ) with the EASJ before 1990 (figure 4(c)) but emerged with strong correlations after 1990 (figure 4(d)). Regardless, the SSP exhibits significant correlations with the EASJ, underlining the co-variability between southeastern China and Bengal (figures 4(e) and (f)).

The EASJ acts as a bridge, linking the local circulations in southeastern China and Bengal, ultimately influencing the development of SSP. Spring







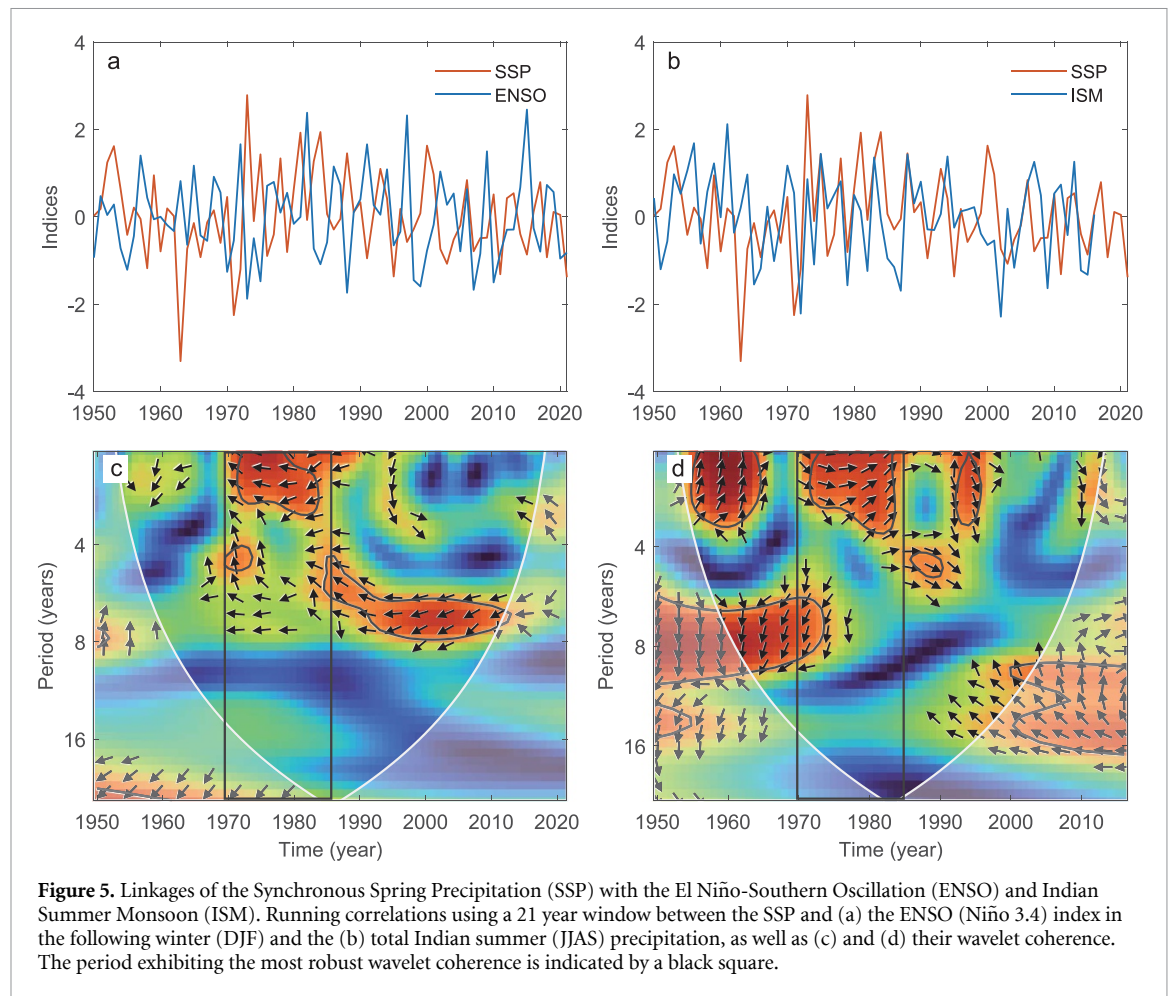
precipitation in southeastern China, situated on the western flank of the western Subtropical Pacific High, shows positive correlations with the southerly winds from the ocean (figures S5–S9), agreeing with previous findings (Tian and Yasunari 1998, Chen *et al* 2014, 2023). This demonstrates that a stronger western Subtropical Pacific High intensifies southerly winds, enhancing moisture transport towards southeastern China, leading to increased spring precipitation (He *et al* 2015, Zhang *et al* 2022). Meanwhile, in Bengal, the prevailing low-level anticyclonic pattern originates in the Bay of Bengal, moving eastward until it encounters the Hengduan Mountains and then deflects westward along the southern Himalayas (figures S5–S9). This anticyclonic flow, obstructed by the complex topography of the Himalayas and Hengduan Mountains, leads to

minimal spring precipitation in the adjacent northern Himalayas and the eastern side of the Hengduan Mountains (figure 1).

### 3.2. Linkages among the ENSO, SSP and ISM

A distinct positive correlation between SSP and the ISM is evident, especially during the period spanning the 1970s to the early 1980s (figures 5(b) and (d)). Interestingly, this period of strong correlation between SSP and ISM aligns with the era that shows the most robust correlations between SSP and the ENSO, as shown in figures 5(a) and (c).

To test whether the SSP-ISM association is stably controlled by the SSP-ENSO linkage over a long period, we reconstructed SSP data dating back to 1796 through the use of tree rings (figure 6(a)). For the reconstruction, we selected thirteen tree-ring



chronologies (table S1) based on their significant ( $p < 0.1$ ) correlation with SSP from 1950 to 1990. Two principal components (PC1 and PC2) derived from these chronologies were used to reconstruct SSP dating back to 1796, capturing 31.6% of the instrumental variance (figure 6(a)). Verification statistics support the robustness of the reconstruction model (Sign Test: 30+/11-; Reduction of Error = 0.25; Product Mean = 3.73). The reconstructed SSP data indicate that current fluctuations in SSP fall within the historical ranges. For example, the driest period from 1926 to 1930 coincides with a dry spell in northern China and a failure of the ISM, which has been linked to the accelerated warming of the 20th century (Liang *et al* 2006, Cook *et al* 2010, Hegerl *et al* 2018). India has relatively long historical climate records compared to eastern Asia (Cook *et al* 2010), and all Indian rainfall indices since 1871 were employed to represent the historical ISM. Indeed, the time-varying SSP-ISM linkages is strong in periods with strong SSP-ENSO correlations over the longer reconstruction period for both the typical eastern Pacific ENSO and central Pacific ENSO (figure 6(b)).

To further examine the controlling factor on the interdecadal shifts of the SSP-ISM relationships, we calculated the correlations between the time series of the SSP-ISM running correlations and the Sea

Surface Temperature (SST) (figure 6(c)). We found that the interdecadal SSP-ISM correlations are positively linked to a pattern resembling the North Pacific Meridional Mode (NPM) (Chiang and Vimont 2004). This association is further supported by a significant correlation with the NPM wind index (figure S4). This suggests that SSP's predictive capacity for the ISM is enhanced when it aligns with the ENSO during the positive phase of NPM.

## 4. Discussion

### 4.1. Regime shift of the SSP in around 1990

The SSP between southeastern China and Bengal is connected primarily relies on the high-level EASJ, which leads to convergence and sustained precipitation in both southeastern China and Bengal as revealed herein and previously (Wan and Wu 2007, Wang *et al* 2017). In addition, a wave train has been observed along the subtropical jet streams, influencing low-level convective activities (Ding and Wang 2005). This interplay of high-level atmospheric patterns plays a vital role in connecting the distinctive low-level spring circulations observed in southeastern China and Bengal. Unlike the SSP observed between southeastern China and Bengal, previous research pointed to a contrasting dipole spring precipitation

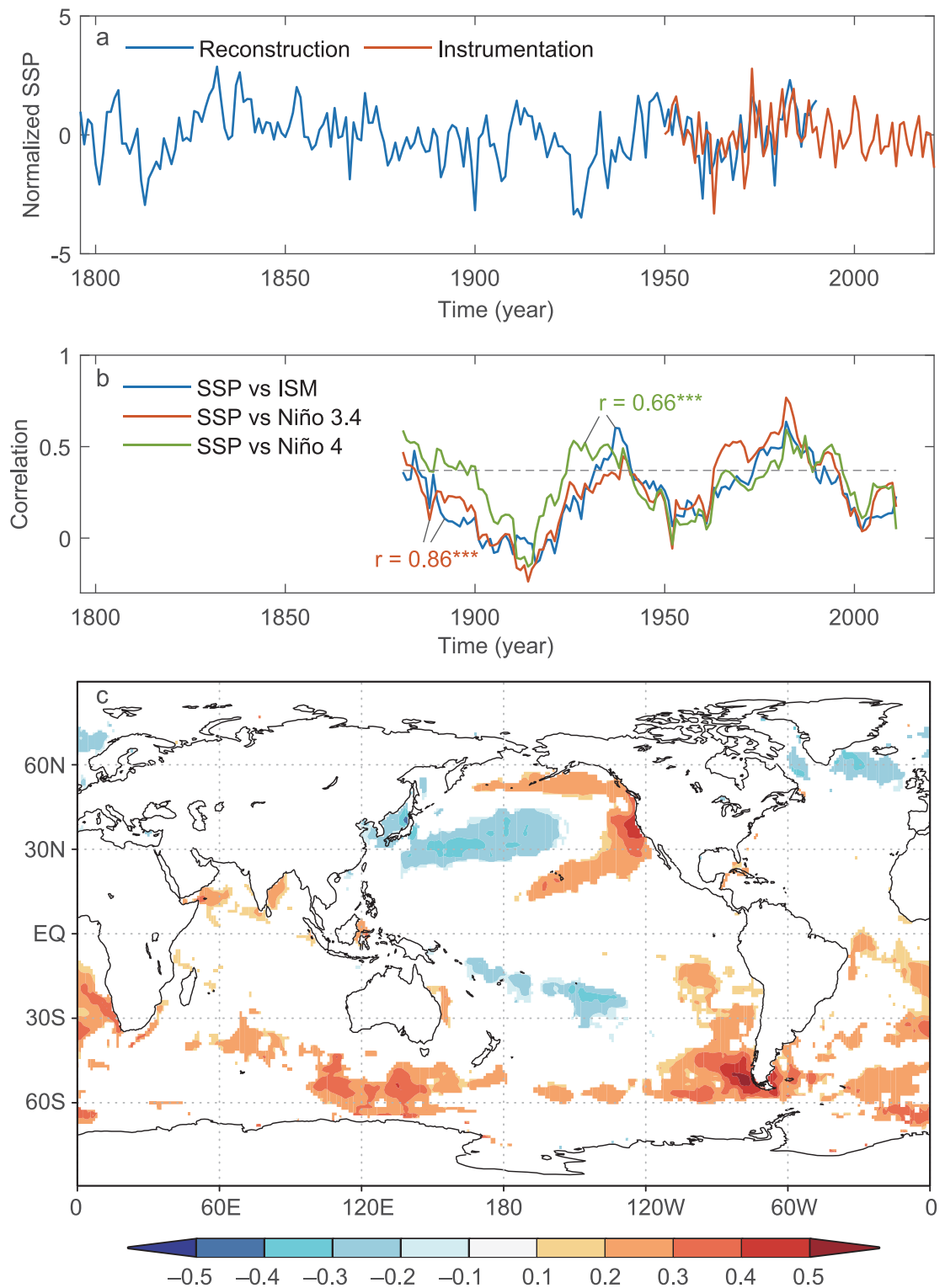


**Figure 6.** Reconstruction of Synchronous Spring Precipitation (SSP) reconstruction and its interplay with the El Niño-Southern Oscillation (ENSO) and Indian Summer Monsoon (ISM). (a) Comparisons of the reconstructed and observed SSP data, (b) 21 year running correlations among the SSP, ISM, Niño 3.4 and Niño 4 and (c) spatial correlation between the time-series of the SSP-ISM running correlation and the annual sea surface temperature (SST). The SSP-Niño 3.4 and SSP-Niño 4 correlations were reversed to facilitate visual comparison. Post-1950 SSP data utilized for computing running correlations were substituted with observational data. The correlations between two running correlation series are 0.86 (SSP-ISM vs SSP-Niño 3.4) and 0.66 (SSP-ISM vs SSP-Niño 4), with a significant level of 0.001. For the 21 year spell, correlation coefficients greater than 0.37 (dashed line) represent significance at the 0.05 level (one-tailed).



pattern between southeastern Tibetan Plateau and southeastern China (Zuo *et al* 2012, Fang *et al* 2021). These seemingly opposite results to our study are due to their focus on a larger study area. In fact, there are also significant regional differences in spring precipitation in Bangladesh and nearby areas of the southeastern Tibetan Plateau (Fang *et al* 2010, Sun *et al* 2023).

Around 1990, the key regions associated with the SSP signal notably shifted from southeastern China to Bengal, as evidenced by higher correlations with southeastern China precipitation before 1990, and with Bengal precipitation after 1990 (figure 3). Our findings emphasize that when Bengal becomes the dominant influence over the SSP, the SSP shows strong correlations with the EASJ extends from Bengal to southeastern China.

However, when southeastern China takes precedence, strong correlations are observed over the eastern part of the EASJ. Before 1990, the eastern branch of the EASJ is relatively strong and thus the SSP is mainly linked to the precipitation in southeastern China to the east (figure S10). This eastern part of the EASJ is linked with a strengthened West Pacific teleconnection (Linkin and Nigam 2008), as evidenced by positive correlations with the western Pacific Subtropical High and negative correlations with the Geopotential Height over the north-central Pacific Ocean (figures S8 and S9). The enhanced linkages between the EASJ and spring precipitation in Bengal after 1990 may be related to the strengthening of the western section of EASJ (figure S10). The EASJ is located over the northern ridge of the western Pacific Subtropical High. After the 1990, the frequent occurrences of the central Pacific ENSO and the westward shift of western Pacific Subtropical High, resulting in strong influences ISM domain climate as revealed previously (Huang *et al* 2018, Li and Wang 2013). This is evidenced in our study by strength correlations with the ENSO (figure S11) and ISM domain climate (figures S5–S9) after 1990.

The regime transition in around 1990 may also be associated with factors such as diminishing Eurasian snow cover that affects atmospheric circulation anomalies, and changes in dominant SST areas that influence precipitation anomalies (Zuo *et al* 2012, Zhu *et al* 2014, Tang *et al* 2022). The modulation of the EASJ is influenced not only by the downstream West Pacific teleconnection but also by the upstream North Atlantic Oscillation (NAO) (Hurrell and Deser 2010), as supported by the marked correlations of the SSP with the Azores High and Icelandic Low (figures S8 and S9). The exact factors responsible for the regime change likely multifaceted and complex. This may also link with phase shifts in the Interdecadal Pacific Oscillation and Atlantic Multidecadal Oscillation (Cai *et al* 2024). Future

research efforts could explore the potential roles of these factors in driving the observed regime shift in SSP.

#### 4.2. SSP as an indicator of ISM

ENSO is a key factor in projecting ISM trends via the Walker circulation, which changes through time along with shifts in the downward limb of the Walker circulation and changes in the ENSO variability (Kumar *et al* 1999, Li *et al* 2013, Xu *et al* 2023). Moreover, the regional Hadley circulation and Indian Ocean SST anomalies also modulate the influence of ENSO on the strength and position of ISM (Cherchi and Navarra 2012, Yu *et al* 2021). The uncertainty in ENSO predictability during spring, which is referred to as the spring predictability barrier (Lai *et al* 2018), further complicates predictions of the ISM based on the persistence of ENSO from spring to summer and the ENSO-ISM relationship. This highlights the intricate nature of monsoon forecasting and the other precursors in spring to predict the behavior of the ISM.

The linkages between SSP and spring precipitation in southeastern China and Bengal primarily occurs on scales of 4–10 years (figures 3(c) and (d)). This timescale partially overlaps with the ENSO period (2–7 years), suggesting a potential link between ENSO and SSP. Indeed, ENSO plays a pivotal role in affecting both SSP and ISM, acting as a bridge between these two systems (Li *et al* 2013, Chen *et al* 2023). An observed decrease in SSP (since 1970s,  $p < 0.05$ ) can potentially signal a northward shift of the summer monsoon, making it a potential predictor for the ISM. Evidence of the enhanced predictive power of SSP on ISM is underscored by a notably stronger correlation between SSP and ISM ( $r = 0.27$ ,  $p < 0.05$ ) than between spring ENSO and ISM ( $r = -0.11$ ,  $p > 0.1$ ). Interestingly, positive correlations between the SSP and the eastern equatorial Pacific SST are observed in the preceding winter, which weaken in concurrent spring and reverse to negative correlations in the subsequent winter (figure S12). ENSO typically develops from the prior spring to the following spring and summer with a persistent pattern, while the ENSO in the decaying phase in winter often shift to the negative phase in the following year (Li *et al* 2014). According to the evolution phase of the ENSO, the SSP is positively with the ENSO in its decaying phase and negatively correlated in its developing phase. The warm ENSO SST anomalies can lead to an anomalous low-level anticyclone over the western North Pacific in the decaying spring. This anticyclonic flow enhances the southwesterly winds, which in turn increases moisture transport and precipitation in southeastern China and Bengal (Xu *et al* 2021). While previous research emphasized positive correlations between SSP and the decaying

phase of ENSO (Wu and Mao 2016), our focus leans toward the developing phase due to its strengthened correlations.

The robust persistence observed in ENSO's developing phase means that the SSP-ENSO connection often extends into summer, consequently influencing both ENSO and ISM. The NPMm emerges as a precursor to ENSO, peaking in spring (Amaya 2019, Jia et al 2021, Hari et al 2022). Moreover, the impact of the spring PMM on the following winter ENSO has been increasing over the past 70 years (Zheng et al 2023). With NPMm in its positive phase, the seasonal coherence within the Indo-Pacific climate among NPMm, ENSO, and ISM strengthens, potentially enhancing the predictability from SSP to ISM.

Spring precipitation in southeastern China is also influenced by the South China Sea summer monsoon. This monsoon typically starts in May, marking a significant climatic shift for the region (Hu et al 2022). Beyond the timing of its onset, interannual variations in the intensity of the summer monsoon also impact spring precipitation. Notably, El Niño events can delay the onset of the summer monsoon, leading to reduced spring rainfall in southeastern China. Conversely, La Niña events often bring an earlier and stronger summer monsoon, resulting in increased spring precipitation (Hu et al 2020, Choi 2021).

## 5. Conclusions

This research provides valuable insights into the SSP in southeastern China and Bengal and its potential as an indicator for the ISM. The co-variability of SSP is intricately linked with the EASJ. Prior to 1990, the EASJ primarily influenced spring precipitation in southeastern China, giving its dominance over SSP. However, Bengal's precipitation became more predominantly influenced by the EASJ and associated SSP after 1990. The predictive capability of SSP for ISM depends on its connections with ENSO. Particularly during the 1970s and early 1980s, when the linkage between SSP and ENSO intensified, the relationship between SSP and ISM was solidified. Our extended reconstruction of SSP dating back to 1796 demonstrates that the connections among SSP, ISM, and ENSO remain consistent over this extended period. This consistency suggests the potential for predicting ISM from SSP, especially when the relationship between SSP and ENSO strengthens during the positive phase of the NPMm. While our study provides valuable insights, further research utilizing coupled models and paleoclimate data is crucial for a more comprehensive understanding of the underlying mechanisms and the long-term predictive power of SSP for the ISM.

## Data availability statement


The data that support the findings of this study are openly available at the following URL/DOI: <https://crudata.uea.ac.uk/cru/data/hrg/>; [www.metoffice.gov.uk/hadobs/hadisst/](http://www.metoffice.gov.uk/hadobs/hadisst/); [www.tropmet.res.in](http://www.tropmet.res.in); <https://cds.climate.copernicus.eu/cdsapp#!/dataset/reanalysis-era5-pressure-levels?tab=overview>; [www.nccei.noaa.gov/products/paleoclimatology/tree-ring](http://www.nccei.noaa.gov/products/paleoclimatology/tree-ring); [www.aos.wisc.edu/~dvmont/MModes/Data.html](http://www.aos.wisc.edu/~dvmont/MModes/Data.html).

## Acknowledgments

This study was funded by the by the National Science Foundation of China (41988101, 42101082, 42301058 and 42130507) and the Swedish STINT (CH2020-8767). We acknowledge the dendrochronologists for their contributions to share the tree-ring data to the ITRDB.

## ORCID iDs

Keyan Fang  <https://orcid.org/0000-0002-0207-0112>

Deliang Chen  <https://orcid.org/0000-0003-0288-5618>

## References

- Amaya D J 2019 The Pacific meridional mode and ENSO: a review *Curr. Clim. Change Rep.* **5** 296–307
- Cai Q, Chen W, Chen S, Xie S-P, Piao J, Ma T and Lan X 2024 Recent pronounced warming on the Mongolian Plateau boosted by internal climate variability *Nat. Geosci.* **17** 181–8
- Chen J, Wen Z, Wu R, Chen Z and Zhao P 2014 Interdecadal changes in the relationship between Southern China winter-spring precipitation and ENSO *Clim. Dyn.* **43** 1327–38
- Chen Y, Wang C, Zhou F, Jiang S, Li X, Weng S, Wan X, Xiao R, Liu Q and Fang K 2023 Weakened western Pacific teleconnection pattern caused a decrease in spring persistent rainfall in north of 26° N over Southeast China *Int. J. Climatol.* **43** 4337–46
- Cherchi A and Navarra A 2012 Influence of ENSO and of the Indian Ocean dipole on the Indian summer monsoon variability *Clim. Dyn.* **41** 81–103
- Chiang J C and Vimont D J 2004 Analogous Pacific and Atlantic meridional modes of tropical atmosphere–ocean variability *J. Clim.* **17** 4143–58
- Choi J-W 2021 An inverse relationship between South China Sea summer monsoon intensity and ENSO *Tellus A* **73** 1–10
- Cook E R 1985 A time series analysis approach to tree ring standardization *PhD The University of Arizona*
- Cook E, Anchukaitis K J, Buckley B M, D'arrigo R D, Jacoby G C and Wright W E 2010 Asian monsoon failure and megadrought during the last millennium *Science* **328** 486–9
- Ding Q and Wang B 2005 Circumglobal Teleconnection in the Northern Hemisphere Summer *J. Clim.* **18** 3483–505
- Fang K et al 2021 ENSO modulates wildfire activity in China *Nat. Commun.* **12** 1764
- Fang K, Gou X, Chen F, Li J, D'arrigo R, Cook E, Yang T and Davi N 2010 Reconstructed droughts for the southeastern Tibetan Plateau over the past 568 years and its linkages to

- the Pacific and Atlantic Ocean climate variability *Clim. Dyn.* **35** 577–85
- Frank D, Fang K and Fonti P 2022 Dendrochronology: fundamentals and innovations *Stable Isotopes in Tree Rings: Inferring Physiological, Climatic and Environmental Responses* ed W Siegwolf, J R Brooks, J Roden and M Saurer (Springer)
- Grinsted A, Moore J C and Jevrejeva S 2004 Application of the cross wavelet transform and wavelet coherence to geophysical time series *Nonlinear Process. Geophys.* **11** 561–6
- Hari V, Ghosh S, Zhang W and Kumar R 2022 Strong influence of north Pacific Ocean variability on Indian summer heatwaves *Nat. Commun.* **13** 5349
- Harris I, Osborn T J, Jones P and Lister D 2020 Version 4 of the CRU TS monthly high-resolution gridded multivariate climate dataset *Sci. Data* **7** 109
- He C, Zhou T, Lin A, Wu B, Gu D, Li C and Zheng B 2015 Enhanced or weakened Western North Pacific subtropical high under global warming? *Sci. Rep.* **5** 16771
- Hegerl G C, Brönnimann S, Schurer A and Cowan T 2018 The early 20th century warming: anomalies, causes, and consequences *Wiley Interdiscip. Rev.: Clim. Change* **9** e522
- Hersbach H et al 2023 ERA5 hourly data on single levels from 1940 to present Copernicus climate change service (C3S) climate data store (CDS)
- Hu P, Chen W, Chen S, Liu Y and Huang R 2020 Extremely early summer monsoon onset in the South China Sea in 2019 following an El Niño event *Mon. Weather Rev.* **148** 1877–90
- Hu P, Chen W, Li Z, Chen S, Wang L and Liu Y 2022 Close linkage of the South China Sea summer monsoon onset and extreme rainfall in may over Southeast Asia: role of the synoptic-scale systems *J. Clim.* **35** 4347–62
- Huang D-Q, Zhu J, Zhang Y-C, Wang J and Kuang X-Y 2015 The impact of the East Asian subtropical jet and polar front jet on the frequency of spring persistent rainfall over southern China in 1997–2011 *J. Clim.* **28** 6054–66
- Huang Y, Wang B, Li X and Wang H 2018 Changes in the influence of the western Pacific subtropical high on Asian summer monsoon rainfall in the late 1990s *Clim. Dyn.* **51** 443–55
- Huijun W, Feng X and Guangqing Z 2002 The spring monsoon in south china and its relationship to large-scale circulation features *Adv. Atmos. Sci.* **19** 651–64
- Hurrell J W and Deser C 2010 North Atlantic climate variability: the role of the North Atlantic oscillation *J. Mar. Syst.* **79** 231–44
- Jia F, Cai W, Gan B, Wu L and Di Lorenzo E 2021 Enhanced North pacific impact on El Niño/southern oscillation under greenhouse warming *Nat. Clim. Change* **11** 840–7
- Kakade S and Kulkarni A 2016 Prediction of summer monsoon rainfall over India and its homogeneous regions *Meteorol. Appl.* **23** 1–13
- Kumar K K, Rajagopalan B and Cane M A 1999 On the weakening relationship between the Indian monsoon and ENSO *Science* **284** 2156–9
- Lai A W-C, Herzog M and Graf H-F 2018 ENSO forecasts near the spring predictability barrier and possible reasons for the recently reduced predictability *J. Clim.* **31** 815–38
- Li F and Wang H 2013 Spring surface cooling trend along the East Asian coast after the late 1990s *Chin. Sci. Bull.* **58** 3847–51
- Li J et al 2013 El Niño modulations over the Past Seven Centuries: amplitude, teleconnection, and the volcanic effect *Nat. Clim. Change* **3** 822–6
- Li J, Xie S P and Cook E 2014 El Niño phases and modes embedded in Asian and North American drought reconstructions *Quat. Sci. Rev.* **85** 20–34
- Li Z, Luo Y, Du Y and Chan J C 2020 Statistical characteristics of pre-summer rainfall over South China and associated synoptic conditions *J. Meteorol. Soc. Japan. II* **98** 213–33
- Liang E, Liu X, Yuan Y, Qin N, Fang X, Huang L, Zhu H, Wang L and Shao X 2006 The 1920s drought recorded by tree rings and historical documents in the semi-arid and arid areas of northern China *Clim. Change* **79** 403–32
- Linkin M E and Nigam S 2008 The North Pacific oscillation—west Pacific teleconnection pattern: mature-phase structure and winter impacts *J. Clim.* **21** 1979–97
- Lorenz E N 1956 *Empirical Orthogonal Functions and Statistical Weather Prediction* (Massachusetts Institute of Technology, Department of Meteorology Cambridge)
- Luo Y, Xia R and Chan J C 2020 Characteristics, physical mechanisms, and prediction of pre-summer rainfall over South China: research progress during 2008–2019 *J. Meteorol. Soc. Japan. II* **98** 19–42
- Michaelson J 1987 Cross-validation in statistical climate forecast models *J. Appl. Meteorol. Climatol.* **26** 1589–600
- Rayner N A, Parker D E, Horton E B, Folland C K, Alexander L V, Rowell D P, Kent E C and Kaplan A 2003 Global analyses of sea surface temperature, sea ice, and night marine air temperature since the late nineteenth century *J. Geophys. Res.* **108** 4407
- Sun W, Wu G, Liu Y, Mao J, Zhuang M and Liu X 2023 Delayed response of the onset of the summer monsoon over the Bay of Bengal to land–sea thermal contrast *J. Clim.* **36** 4051–70
- Tang W, Fu Y, Wang X, Lu Y, Xu M, Xie W and Song A 2022 Decreasing spring persistent rainfall over the Yangtze-Huai River Valley of China during 1960–2019 and its possible causes *Int. J. Climatol.* **42** 3809–19
- Tian S-F and Yasunari T 1998 Climatological aspects and mechanism of spring persistent rains over central China *J. Meteorol. Soc. Japan. II* **76** 57–71
- Trenberth K E and Stepaniak D P 2001 Indices of el Niño evolution *J. Clim.* **14** 1697–701
- Wan R and Wu G 2007 Mechanism of the spring persistent rains over southeastern China *Sci. China D* **50** 130–44
- Wang B and Ding Q 2008 Global monsoon: dominant mode of annual variation in the tropics *Dyn. Atmos. Oceans* **44** 165–83
- Wang P X, Wang B, Cheng H, Fasullo J, Guo Z, Kiefer T and Liu Z 2017 The global monsoon across time scales: mechanisms and outstanding issues *Earth Sci. Rev.* **174** 84–121
- Wang S, Hou Y, Zhou S, Zuo H, Sun F and Luo -J-J 2021 Effect of circulation variation associated with East Asian jet on spring rainfall over North China and Yangtze-Huaihe River Valley *Atmos. Res.* **258** 105611
- Wu X and Mao J 2016 Interdecadal modulation of ENSO-related spring rainfall over South China by the Pacific decadal oscillation *Clim. Dyn.* **47** 3203–20
- Xu B, Li G, Gao C, Yan H, Wang Z, Li Y and Zhu S 2021 Asymmetric effect of El Niño—Southern oscillation on the spring precipitation over South China *Atmosphere* **12** 391
- Xu C, Wang S-Y S, Borhara K, Buckley B, Tan N, Zhao Y, An W, Sano M, Nakatsuka T and Guo Z 2023 Asian-Australian summer monsoons linkage to ENSO strengthened by global warming *npj Clim. Atmos. Sci.* **6** 8
- Yu S Y, Fan L, Zhang Y, Zheng X T and Li Z 2021 Reexamining the Indian summer monsoon rainfall–ENSO relationship from its recovery in the 21st century: role of the Indian ocean SST anomaly associated with types of ENSO evolution *Geophys. Res. Lett.* **48** e2021GL092873
- Zhang F, Yang X, Sun Q, Yao S and Guo Q 2022 Three-dimensional structural anomalies of the Western Pacific subtropical high ridge and its relationship with precipitation in China during August–September 2021 *Atmosphere* **13** 1089
- Zheng Y, Chen S, Chen W and Yu B 2023 A continuing increase of the impact of the spring North Pacific meridional mode on the following winter El Niño and Southern oscillation *J. Clim.* **36** 585–602
- Zhu Z, Li T and He J 2014 Out-of-phase relationship between boreal spring and summer decadal rainfall changes in southern China *J. Clim.* **27** 1083–99
- Zuo Z, Zhang R and Wu B 2012 Inter-decadal variations of springtime rainfall over southern China mainland for 1979–2004 and its relationship with Eurasian snow *Sci. China Earth Sci.* **55** 271–8